THE JOURNAL OF PHYSICAL CHEMISTRY B

ARTICLE

pubs.acs.org/JPCB

# Accurate Static and Dynamic Properties of Liquid Electrolytes for Li-Ion Batteries from ab initio Molecular Dynamics

P. Ganesh*

Center for Nanophase Materials Sciences, Oak Ridge National Laboratory, Oak Ridge, Tennessee 37831, United States

De-en Jiang

Chemical Sciences Division, Oak Ridge National Laboratory, Oak Ridge, Tennessee 37831, United States

P. R. C. Kent

Center for Nanophase Materials Sciences, Oak Ridge National Laboratory, Oak Ridge, Tennessee 37831, United States

**ABSTRACT:** Lithium-ion batteries have the potential to revolutionize the transportation industry, as they did for wireless communication. A judicious choice of the liquid electrolytes used in these systems is required to achieve a good balance among high-energy storage, long cycle life and stability, and fast charging. Ethylene-carbonate (EC) and propylene-carbonate (PC) are popular electrolytes. However, to date, almost all molecular-dynamics simulations of these fluids rely on classical force fields, while a complete description of the functionality of Li-ion batteries will eventually require quantum mechanics. We perform accurate ab initio molecular-dynamics simulations of ethylene- and propylene-carbonate with $LiPF_6$ at experimental concentrations to build solvation models which explain available neutron scattering and nuclear magnetic resonance (NMR) results and to compute Li-ion solvation energies and diffusion constants. Our results suggest some similarities between the two liquids as well as some important differences. Simulations also provide useful insights into formation of solid-electrolyte interphases in the presence of electrodes in conventional Li-ion batteries.

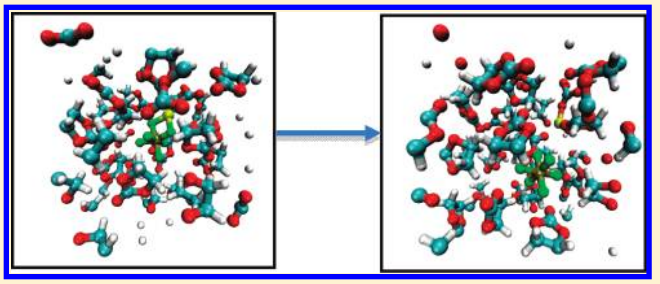

## INTRODUCTION

The study of liquid electrolytes is of great interest both theoretically and experimentally. In the last few decades, one of the main reasons for studying these systems has been to obtain a better understanding of Li-ion batteries[1,2] and fuel cells.[3] In both of these systems, electrolytes act as the medium through which ions diffuse from one electrode to the other, thereby converting chemical energy to electrical energy. The structure and dynamics of a wide range of salts in aprotic electrolytes and their mixtures have been studied experimentally using a broad range of techniques such as X-ray scattering,[4−6] neutron scattering,[7] Raman and infrared spectroscopy,[8,9] nuclear-magnetic resonance,[10,11] etc. Correlating these observations with electrochemical measurements demonstrates that the type of solvent used affects the solvation and diffusion of Li, which in turn affects the ionic conductivity and hence the whole performance of the Li-ion battery cell, especially its power density. In principle, every component of the electrochemical cell can be separately optimized to determine the theoretical and practical performance limits.

Li-ion battery is an electrochemical cell where inside the cell charge is carried by Li-ions. As such, the faster the Li-ions diffuse, the greater the current density, thereby increasing the power rating of the cell. Each electrolyte has its own potential stability window, with a typical maximum of ∼4.6 V. In addition, popular electrolytes, such as ethylene-carbonate (EC), dimethyl-carbonate (DMC), and propylene-carbonate (PC) are prone to degradation with every charge−discharge cycle. The decomposed products usually form a solid layer, the solid-electrolyte interphase (SEI) layer,[12] at the electrolyte−electrode interface, thereby acting as a bottleneck to charge and mass-transfer across the electrodes. Due to their insulating nature, SEIs are nevertheless thought to be useful in reducing reductive decomposition of the electrolyte but form the most resistive part of the battery.[13] To date, no overall clear understanding exists of the actual mechanism, energetics, and time scales by which Li becomes solvated to Li-ion in aprotic solution and diffuses to intercalate in the electrodes. As such, the formation and role of the SEI layer is not well understood either.[12] This hinders the process of designing better electrolytes which would have a higher operating potential range and would also allow for a high Li-ion diffusivity,

**Received:** January 12, 2011
**Published:** March 09, 2011

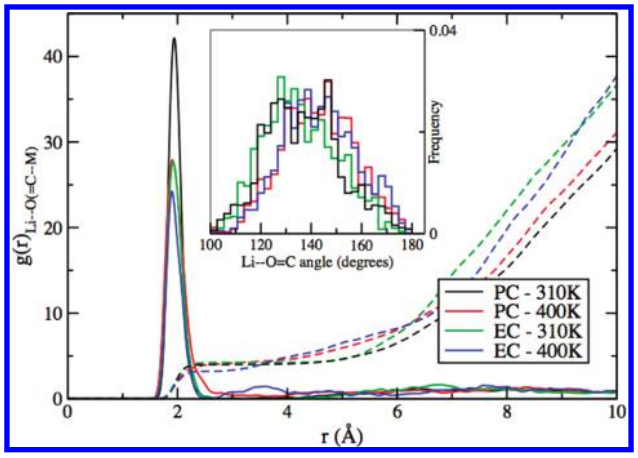


**Figure 1.** Partial radial-distribution function of Li-ion with the carbonyl oxygen of EC and PC along with the partial-density weighted integral (dashed lines) which equals the Li-ion coordination number. In both the electrolytes, the Li−O(carbonyl) distance is ∼2 Å, and the first-solvation shell of Li-ion has 4 EC or PC molecules consistent with experiments. Inset shows the histogram of the Li−O=C angle.

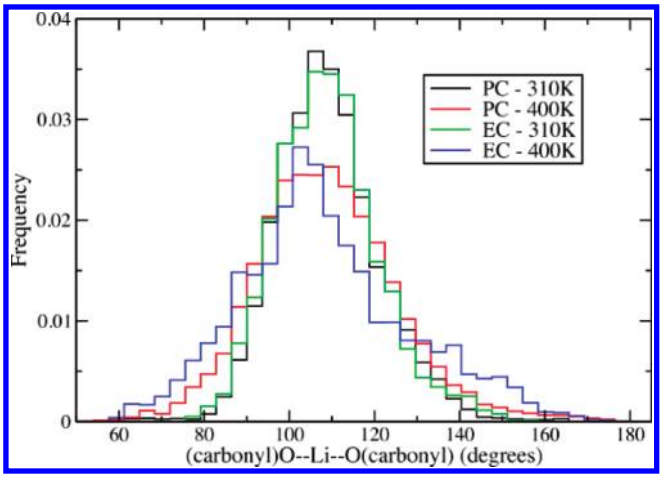


**Figure 2.** Histogram of the (carbonyl)O−Li−O(carbonyl) angle showing a peak ∼110°, suggesting that $Li^+$ is tetrahedrally coordinated to four solvent molecules.

thereby increasing the low power density that plagues current Li-ion batteries.

Most of the simulations to date have used classical potentials or force fields,[14−16] parametrized to capture selected properties of the system.[17−20] This has resulted in contrasting pictures of Li-ion solvation and ion association in carbonate solvents in the literature.[8,17,18] Knowing the Li-ion solvation sheath is important in understanding the anode chemistry.[21] A parameter-free method, which can reproduce the equilibrium static and dynamic properties of the electrolytic system as well as capture relevant reactions, is required to achieve computational design of electrolytes for battery applications. Only recently has a single communication[22] been made which attempts to model the initial stages of the SEI formation on the graphitic anode of Li-ion batteries using ab initio methods. The calculations show the importance of using first-principles based methods which explicitly treat the quantum-natured electrons and are parameter-free to model the interfacial chemistry under charging and discharging conditions. Although simulations of electrolyte structure using classical potentials are well justified, the potentials do not allow for any type of new chemistry either in the bulk or at the electrolyte−electrode interface. However, to a large extent it is the interfacial chemistry, such as SEI formation, that determines the overall functionality of a battery. This chemistry is in principle captured by ab initio methods, giving them a potential key role in understanding the interfacial chemistry and in the design of improved devices.

In this paper we report ab initio MD simulations of $LiPF_6$ in two contrasting electrolytes, ethylene-carbonate (EC) and propylene-carbonate (PC), to determine for the first time accurate solvation models for Li-ion, diffusion coefficients, and Li-solvation energies.

## ■ RESULTS AND DISCUSSIONS

Figure 1 shows the partial radial-distribution function of Li-ion with the carbonyl oxygen of EC and PC at two different simulated temperatures (310 and 400 K), determined from our MD simulations. Bader charge analysis[23] of representative atomic structures revealed that solvated lithium in EC and PC essentially exists as a positive ion. The solvated Li-ion effectively bonds with the carbonyl-oxygens of the solvent. The near-neighbor Li−O(carbonyl) distance is about ∼1.94 Å (∼1.90 Å) in PC at 310 K (400 K). Time of flight neutron scattering experiments[7] have measured the Li−O(carbonyl) near-neighbor distance to be ∼2.04 Å for PC at room temperature, in good agreement with our simulation results. The Li−O(carbonyl) peak height in the smaller EC molecule is ∼1.92 Å (∼1.90 Å) at 310 K (400 K). Surprisingly, irrespective of being a smaller molecule than PC, the Li−O(carbonyl) near-neighbor distances are very similar in both. This is only possible if this distance is mainly dictated by the electrostatic interactions between the two involved species, i.e., Li-ion and the double-bonded carbonyl-oxygen. In comparison, classical force fields provide a range of values from 1.70[18,20] to 1.98 Å,[19] depending on the potential. Interestingly, at 400 K, a broad second maximum develops in EC. This is mainly due to a nonspherical solvation shell at higher temperatures, thus allowing more free volume for the Li-ion inside the shell. The near-neighbor distance between Li-ion and P of $PF_6^-$ is about 6 Å in EC and 9 Å in PC at 310 K. The distance increases to 7.7 Å at 400 K in EC while staying nearly the same in PC.

The inset in Figure 1 shows bond-angle distribution of the Li−O=C(carbonyl) for EC and PC at different temperatures. The full range of the distribution is from 100° to 180°. In PC, the distribution is centered at 140°. This is consistent with the measured value[7] of 138° in PC. In EC, the range is the same, but there is a stronger temperature dependence of the skewness of the distribution. The broad distributions suggest incessant hopping of the Li-ion within its solvation shell. Although the Li−O(carbonyl) near-neighbor distance is captured rather close to the experimental value with rigorous fitting of nonbonded and angular/dihedral potential forms to gas-phase quantum chemistry cluster calculations,[18] the most probable Li−O=C(carbonyl) angle has been reported to be ∼160° for $Li^+$ in EC and PC[18] using classical force-field simulations. In an unmixed salt + solvent mixture a different classical simulation study computed this to be ∼150°.[19] These values are much larger than the experimental value of 138°, which is closer to our ab initio MD results. Figure 2 further shows that the (carbonyl)O−Li−O(carbonyl) angle histogram is centered around ∼110°, suggesting that $Li^+$ is tetrahedrally coordinated by the four solvent molecules in the first coordination shell. There is again a strong temperature dependence seen in both EC and PC.

A partial-density weighted integral of the partial radial-distribution function in Figure 1 shows that the first Li-solvation shell consists of four PC molecules at both 310 and 400 K. For EC, the shape of the solvation shell is temperature dependent. At 310 K, there are four EC molecules in the first shell within ~3 Å. This is consistent with hybrid DFT calculations[24] on $Li^+(EC)_n$ supermolecules, which suggest the largest stable complex has four EC molecules around $Li^+$. However, at 400 K the solvation shell is less spherical, and the first solvation shell is only fully described at ~4 Å. At both temperatures, four EC molecules constitute the first-solvation shell of the Li-ion. The solvation model for PC from neutron scattering studies[7] has 4.5 PC molecules around Li-ion at room temperature, close to our computed value of 4. Given that our concentration is 0.5 M, while the experiment was performed at ~1.5 M salt concentration, the level of comparison is quite good. The Li-solvation shell is found to be very tight; i.e., no exchange of molecules between the first- and the second-solvation shell is seen during the simulation. In contrast, classical MD simulations yielded a solvation shell of 3.6 EC molecules around Li-ion at 298 K;[19] hence, our first-principles MD simulations seem to provide a better description of the solvation environment of Li-ion in EC, in comparison with experiment. We compute the radius of gyration of solvated Li-ion at 310 K to be 4.5 Å in EC and 5.3 Å in PC. We also do not find any $F^-$ ions in the first coordination shell of $Li^+$,[7] consistent with neutron scattering experiments and in contrast to classical MD simulation.[19]

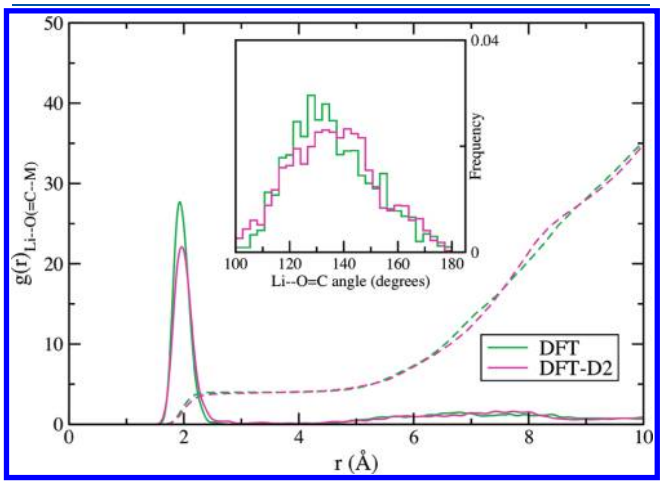


**Figure 3.** Comparison of the partial radial-distribution function of Li with the carbonyl oxygen of EC along with the partial-density weighted integral (dashed lines), which equals the Li coordination number, with van der Waals (DFT-D2) and without (DFT) at 310 K. Inset shows the histogram of the Li−O=C angle.

Conventional DFT method does not explicitly contain van der Waals (dispersion) interactions, which are often thought to be important in describing interactions between organic molecules. To study the effect of van der Waals interactions in the solvation of $Li^+$, we performed an additional simulation of $Li^+$ and $PF_6^-$ in EC at 310 K with a Grimme potential added to the Hamiltonian, with published parameters.[25] The range of the Grimme potential was chosen to be 30 Å, larger than twice the linear dimension of our cell. Figure 3 shows the comparison of the Li−O(carbonyl) partial radial-distribution function and the Li−O=C(carbonyl) bond-angle distribution function for two sets of simulations of roughly equal length, one with Grimme's empirical van der Waals potential (DFT-D2) and one without (DFT). With van der Waals interaction included, the position of the first peak is slightly shifted to the right to 1.96 Å, but the $Li^+$ solvation shell again has four EC molecules. Because the radial distribution is directly related to the negative of the potential-of-mean-force, the drop in the height of the first peak with the inclusion of van der Waals by 5.5 may suggest a slightly weakened Li−O interaction compared to pure DFT. The ion−solvent and the solvent−solvent long-range interactions are not greatly affected by the inclusion of van der Waals forces. The Li−O=C(carbonyl) distribution is also very similar, suggesting that van der Waals interaction has a negligible effect on the structure of the $Li^+$ solvation shell in EC. Given the large charge differences between $Li^+$ and carbonyl-oxygens, this interaction is mainly governed by electrostatics, and as such the weak influence of van der Waals forces on the solvation shell structure might have been expected.

Figure 4 shows the mean-squared displacement of solvated Li-ion and P of $PF_6^-$ in EC and PC. The long-time Stokes−Einstein diffusion coefficient of Li in PC jumps from ~$0.7 \times 10^{-9}$ $m^2/s$ at 310 K to ~$3.7 \times 10^{-9}$ $m^2/s$ at 400 K. The diffusion coefficients of Li-ion in EC at 310 and 400 K are ~$1.0 \times 10^{-9}$ $m^2/s$. At 298 K, experimentally measured diffusion of $LiPF_6$ in PC is $0.4 \times 10^{-9}$ $m^2/s$ in 0.5 M $LiPF_6$/PC,[26] and the bulk diffusion coefficient of 0.5 M $LiPF_6$ in EC[10] is ~$0.62 \times 10^{-9}$ $m^2/s$. The experimentally measured self-diffusion coefficient at salt concentrations similar to those in our simulation at 40 °C of Li-ion in LiTFSI in EC is $0.21 \times 10^{-9}$ $m^2/s$, and at 30° of LiTFSI in PC, it is $0.16 \times 10^{-9}$

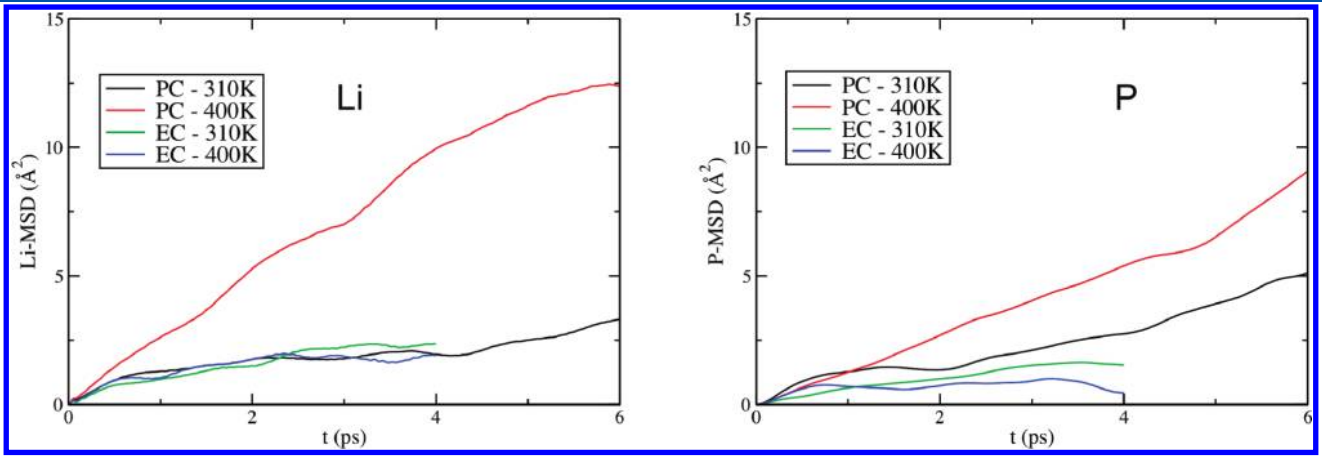


**Figure 4.** Mean-squared displacement of solvated Li-ion and P of $PF_6^-$ in EC and PC.


dx.doi.org/10.1021/jp2003529 |J. Phys. Chem. B 2011, 115, 3085–3090

$m^2/s$,[27] in good comparison to our calculated results. Note that the diffusion of Li-ion in solution is 4−5 orders of magnitude larger than the measured diffusion coefficient of Li intercalated in graphite.[28] The diffusion of P in the $PF_6$ anion shows trends similar to those in Li-ion diffusion in PC. It jumps from $1.2 \times 10^{-9}$ $m^2/s$ at 310 K to $\sim 2.3 \times 10^{-9}$ $m^2/s$ at 400 K. Diffusion in EC is fairly constant and equal to $\sim 0.7 \times 10^{-9}$ $m^2/s$. This shows that in PC the $PF_6^-$ ion diffuses faster than $Li^+$, consistent with recent NMR measurements.[29] The fast diffusion of solvated Li-ion emphasizes the need to form and maintain ions separately in solution. The relatively slower diffusion of $Li^+$ and $PF_6^-$ ions in EC compared to PC again suggests that EC binds to ions more strongly than PC. In fact, in one of our simulations with EC at 310 K (Figure 7), a spontaneous Li-solvation was observed within ∼7 ps, consistent with the high dielectric constant of EC (91 at 309 K[30]). The relatively linear increase in the mean-squared displacement over the time scale of the simulation and the good agreement to NMR measurements of the diffusion coefficient suggest that our ab initio MD runs are long enough to give a good estimate of diffusion coefficients of $Li^+$ and $PF_6^-$ ions. Diffusion coefficients derived from simulations over nanoseconds or greater time scales would definitely be desirable and more accurate, but these are infeasibly long for ab initio calculations.

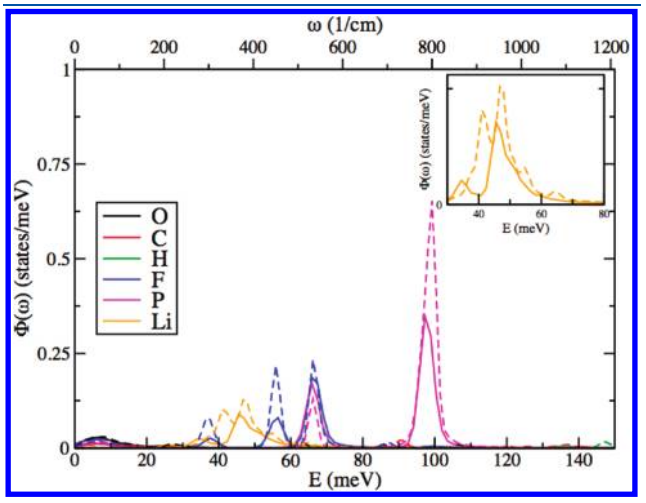


**Figure 5.** Atom-type projected vibrational density-of-states of solvated Li-ion and $PF_6^-$ in PC at 400 K (solid lines) and in EC at 310 K (dashed lines). Inset shows the small peak of Li ∼62 meV.

Figure 5 shows the vibrational density-of-states (VDOS) projected onto different atomic species for $LiPF_6$ in EC at 310 K and in PC at 400 K. This can be compared with inelastic-neutron-scattering (INS) or Raman and infrared-reflectivity measurements. The low-energy acoustic modes appear as a small peak around ∼5 meV for all the species. The largest Li peak is around ∼50 meV in both EC and PC, with the peak splitting being more in PC than in EC. There is also a smaller peak at ∼60−62 meV (inset) which overlaps with that of carbonyl-oxygen. Interestingly, phonon density-of-states from neutron scattering experiments on $Li^+$ intercalated $Li_xCoO_2$[31] also find a broad maximum near 60 meV. This suggests that the Li dynamics and its interaction with oxygen have some similarities

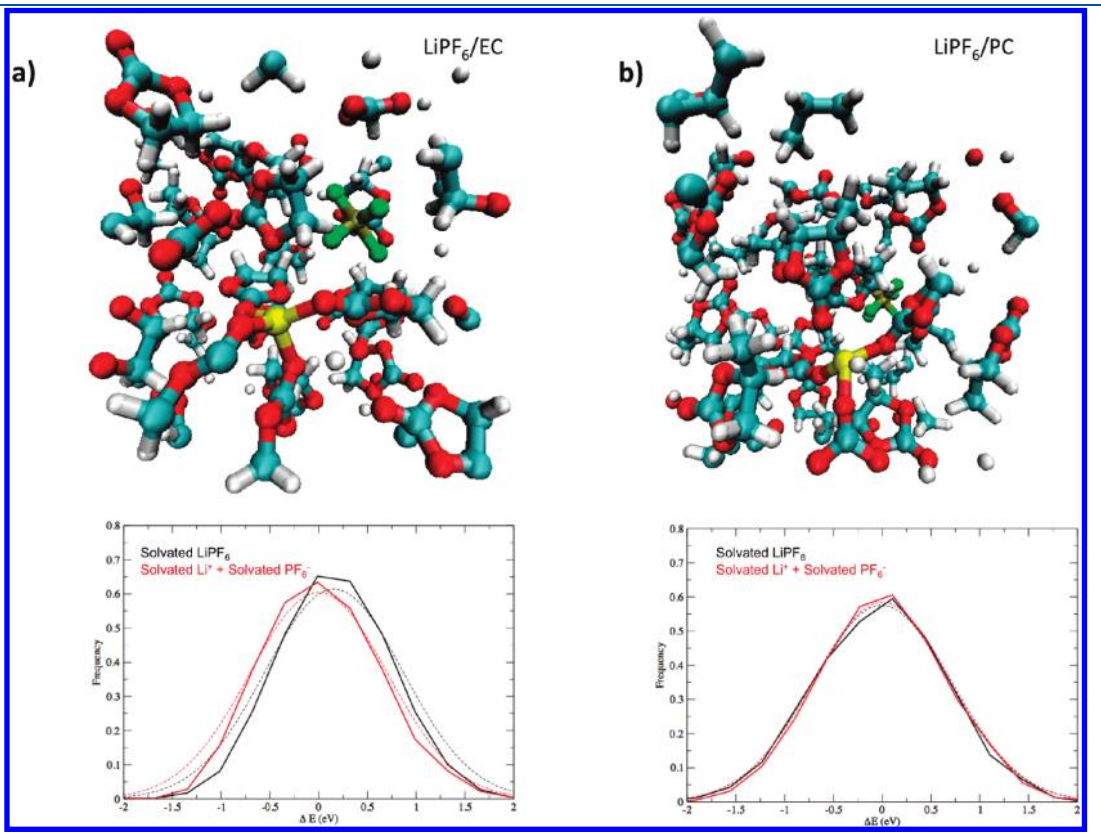


**Figure 6.** (a) and (b) Atomistic solvation models of Li-ion in EC and PC, respectively. Red is oxygen, green is fluorine, blue is carbon, gray is phosphorus, and yellow is lithium. The plots at the bottom show histograms of Kohn−Sham energies for solvated $LiPF_6$ and a pair of solvated $Li^+$ and $PF_6^-$ at 310 K in EC (a) and PC (b), respectively.

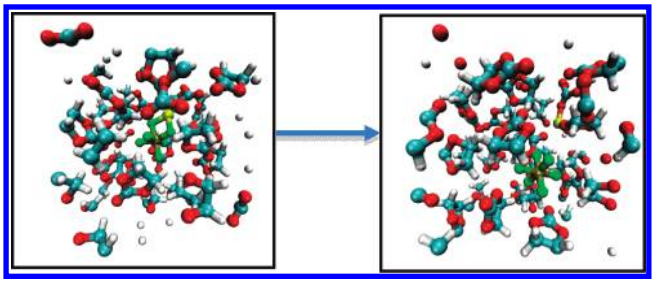

**Figure 7.** Spontaneous dissociation of $LiPF_6$ in EC to solvated $Li^+$ and $PF_6^-$ ions in our AIMD simulation at 310 K.

in both cases. This may explain the ease of $Li^+$ intercalation from liquid-electrolyte into solid electrodes like $Li_xCoO_2$. The computed peak positions compare well with FT-IR and Raman measurements for solid $LiPF_6$[31] as well as $PF_6^-$[32] in solution with several aprotic solvents. Phosphorus has two distinct peaks: one corresponding to a higher-energy diffusive mechanism and the other to a low-energy librational peak which couples strongly with the fluorine peak at ~68 meV. There are two more strong fluorine peaks at ~56 and ~36 meV. In solutions of EC/DMC, peaks are observed at ~837, 561, and 470 $cm^{-1}$,[9] similar to what we find from our computed VDOS. The absence of a phosphorus or fluorine peak at 741 $cm^{-1}$[33] is consistent with having separately solvated $Li^+$ and $LiPF_6$ in our electrolyte solution. All computed peaks are consistently shifted to lower energies, consistent with our solutions having higher permittivity than the 1 M EC/DMC mixtures used in actual experiments.

To compute solvation energies, lengthy (15−25 ps) ab initio runs were performed at 310 K, one with solvated $LiPF_6$ and another with solvated Li-ion and $PF_6^-$ in PC. Similar, but relatively shorter, runs were performed in EC. Figure 6 shows the normalized histograms of the Kohn−Sham energy for the two cases in 26 molecules of EC (a) and PC (b), along with their Gaussian fits (dotted line). In EC, the mean of the histogram for separately solvated $Li^+$ and $PF_6^-$ ions (red curve) is clearly lower than that of solvated $LiPF_6$ by ~0.25 eV. In comparison, the histograms for PC are practically on top of each other. The stark difference in the mean suggests that it is energetically more favorable to solvate Li-ion in EC than it is in PC. Also, the histogram widths in PC are similar to those in EC, consistent with their similar specific-heat values.[34] In fact, in one of our PC runs at 400 K, it was very easy to form a LiF pair, a major constituent of the solid-electrolyte interface in batteries,[1] with no easily distinguishable change in the internal energy. The large solvation energy of Li in EC leads to a spontaneous dissociation of a $LiPF_6$ pair to form solvated Li-ion and $PF_6^-$ within 7 ps at 310 K (Figure 7). No such spontaneous dissociation of the salt is seen in PC, even at 400 K. However, if Li is forced to solvate, then no recombination is seen even after a 25 ps long molecular-dynamics simulation. The ease of Li solvation in EC may be due to its relatively higher dielectric constant than PC.[1,30]

## CONCLUSION

We show the feasibility and effectiveness of performing ab initio molecular-dynamics of liquid electrolytes such as EC and PC with $LiPF_6$. Simulations give accurate structures and solvation models for Li-ion which agrees well with existing neutron scattering experiments. The results are more accurate and consistent than classical simulations[5,18,19] and do not have any adjustable free parameters, beyond the choice of DFT. The effect of van der Waals interactions on the solvation shell structure is shown to be negligible. The solvation energies come out naturally from the simulations. While PC is stable over a wider temperature range (−48.8 to 242 °C), than EC (36.4 to 248 °C), it is a bigger and heavier molecule with a low-temperature glass transition close to ~190 K.[35] At room temperature, EC has a dielectric constant of 89.78, whereas PC has a lower dielectric constant of 64.92, lower even than water. The relatively higher dielectric constant of EC is responsible for keeping the Li-ion solvated more effectively than in PC and avoids reformation of ion pairs. Our computed diffusion constant of solvated Li-ion in EC and PC at 310 K agrees well with measured values at room temperature. The clear jump in Li-ion diffusivity in PC with an increase in temperature from 310 to 400 K suggests that a mixture of PC with other electrolytes such as EC or DMC, which easily form SEI, is better for high-temperature applications than a solvent mixture without PC. Further, the vibrational density-of-states of Li in EC and PC shows peaks at energies similar to those measured experimentally for solid electrolytes such as $LiCoO_2$,[31] suggesting perhaps a similar Li dynamics in both liquid and solid electrolytes, important for an easy Li intercalation into the electrodes. In one of our simulations with EC, a spontaneous solvation of Li-ion was observed only after 7 ps. It is also seen that in PC a LiF pair is very readily formed, a major constituent of solid electrolytes in Li-ion batteries,[21] at 400 K. This suggests that the salt is more likely to dissolve in EC than in PC. Our study acts as a stepping-stone for future atomistic ab initio modeling to understand SEI interphase chemistry and Li-intercalation, both vital for optimizing future battery performance.

## SIMULATION AND ANALYSIS METHODS

We perform ab initio Born−Oppenheimer molecular-dynamics of bulk EC and PC with/without $LiPF_6$ using the Vienna Ab-Initio Simulation Package (VASP).[36] A PBE-GGA exchange-correlation functional was used with Projector Augmented Wave (PAW) potentials.[37,38] The excellent agreement of static structure and diffusion coefficients with available experiments justifies this choice. Simulations were performed at the temperatures of $T$ = 310 K and $T$ = 400 K for 27 molecules of EC (PC) corresponding to densities of 1.356 g/mL (1.205 g/mL), close to the experimental density. A single $LiPF_6$ molecule was substituted for a single EC (PC) molecule corresponding to a salt concentration of 0.55 M (0.45 M). An initial canonical NVT simulation was carried out for all the systems for 10 ps (5 ps) for EC (PC) systems. A spontaneous dissociation of $LiPF_6$ into $Li^+$ and $PF_6^-$ was observed ~7 ps in EC. No such dissociation was seen in PC. As such, the ion-pair was manually separated in PC, followed by a 5 ps NVT run at each temperature. This was followed by a microcanonical NVE run for 15 ps (15 ps) for EC (PC) where the energy drift was ~0.16 meV/fs. For EC, dynamics were initially made with a deuterium mass for protons before switching to hydrogen mass in the last 5 ps of the NVE run. Analysis was performed for the NVE simulations with hydrogen masses for protons. An additional NVE run was performed for ~5 ps with an added Grimme-type dispersion interaction[25] between all species to account for the van der Waals interaction. This was done to study the effect of van der Waals in the solvation of $Li^+$ in EC. Independent long (~25 ps) pure DFT runs were made in PC at 310 K due to its low-temperature slow dynamics, and ensemble averages were taken. The energy histograms in Figure 6 were

obtained from NVT runs at 310 K. A single **k**-point (the Γ point) and a plane-wave cutoff of 300 eV were used. A Nose-thermostat was used for the NVT simulation. Most of the simulations were carried out in our local Beowulf cluster and took 3(2) steps/min for EC(PC) on 32-cores using parallelization over an Inifiniband network.

The partial radial-distribution function, $g_{\alpha\beta}(r)$ was computed using standard definitions, smoothed with a normalized Gaussian of width 0.05 Å. To compute the angular distribution of Li−O═C, a cutoff of 1.2 Å was used for the O═C bond and 2.2 Å for the Li−O bond. Diffusion coefficient, $D$, of Li was obtained from the slope of its mean-squared displacement according to the Stokes−Einstein relation $<(\Delta r)^2> = 6D(\Delta t)$. Velocities obtained along the trajectory were used to compute the velocity-autocorrelation function $Z(t) = (<\mathbf{v}(0)\cdot\mathbf{v}(t)>)/(<\mathbf{v}(0)\cdot\mathbf{v}(0)>)$ for each atomic species, where <..> denotes a time average. A direct Fourier transform of this quantity was defined as $Z(\omega) = (1/(T(2\pi)^{1/2}))\int_0^T dt Z(t)e^{i\omega t}$ to obtain the vibrational density-of-states $\Phi(\omega) = Z^2(\omega)$.

## AUTHOR INFORMATION


### Corresponding Author

*E-mail: gpanchap@gmail.com.


## ACKNOWLEDGMENT

This material is based upon work supported as part of the Fluid Interface Reactions, Structures and Transport (FIRST) Center, an Energy Frontier Research Center funded by the U.S. Department of Energy, Office of Science, Office of Basic Energy Sciences under Award Number ERKCC61. This research also used resources of the National Energy Research Scientific Computing Center, which is supported by the Office of Science of the U.S. Department of Energy under Contract No. DE-AC02-05CH11231

## REFERENCES


(1) Xu, K. *Chem. Rev.* **2004**, *104*, 4303.
(2) Goodenough, J. B.; Kim, Y. *Chem. Mater.* **2010**, *22*, 587.
(3) Winter, M.; Brodd, R. J. *Chem. Rev.* **2004**, *104*, 4245.
(4) Markle, W.; Colin, J. F.; Goers, D.; Spahr, M. E.; Novak, P. *Electrochim. Acta* **2010**, *55*, 4964.
(5) Soetens, J. C.; Millot, C.; Maigret, B.; Bako, I. *J. Mol. Liq.* **2001**, *92*, 201.
(6) Soetens, J.-C.; Millot, C.; Maigret, B.; Bakó, I. *J. Mol. Liq.* **2001**, *92*, 201.
(7) Kameda, Y.; Umebayashi, Y.; Takeuchi, M.; Wahab, M. A.; Fukuda, S.; Ishiguro, S.-i.; Sasaki, M.; Amo, Y.; Usuki, T. *J. Phys. Chem. B* **2007**, *111*, 6104.
(8) Burba, C. M.; Frech, R. *J. Phys. Chem. B* **2005**, *109*, 15161.
(9) Aroca, R.; Nazri, M.; Nazri, G. A.; Camargo, A. J.; Trisc, M. *J. Solution Chem.* **2000**, *29*, 1047.
(10) Yang, L.; Xiao, A.; Lucht, B. L. *J. Mol. Liq.* **2010**, *154*, 131.
(11) Cazzanelli, E.; Mustarelli, P.; Benevelli, F.; Appetecchi, G. B.; Croce, F. *Solid State Ionics* **1996**, *86−8*, 379.
(12) Fong, R.; Vonsacken, U.; Dahn, J. R. *J. Electrochem. Soc.* **1990**, *137*, 2009.
(13) Xu, K. *Energies* **2010**, *3*, 135.
(14) Masia, M.; Probst, M.; Rey, R. *J. Phys. Chem. B* **2004**, *108*, 2016.
(15) Tsunekawa, H.; Narumi, A.; Sano, M.; Hiwara, A.; Fujita, M.; Yokoyama, H. *J. Phys. Chem. B* **2003**, *107*, 10962.
(16) Li, S.; Cao, Z.; Peng, Y. X.; Liu, L.; Wang, Y. L.; Wang, S.; Wang, J. Q.; Yan, T. Y.; Gao, X. P.; Song, D. Y.; Shen, P. W. *J. Phys. Chem. B* **2008**, *112*, 6398.
(17) Borodin, O.; Smith, G. D. *J. Phys. Chem. B* **2006**, *110*, 4971.
(18) Soetens, J.-C.; Millot, C.; Maigret, B. *J. Phys. Chem. A* **1998**, *102*, 1055.
(19) Borodin, O.; Smith, G. D. *J. Phys. Chem. B* **2009**, *113*, 1763.
(20) Li, T.; Balbuena, P. B. *J. Electrochem. Soc.* **1999**, *146*, 3613.
(21) Xu, K.; Lam, Y.; Zhang, S. S.; Jow, T. R.; Curtis, T. B. *J. Phys. Chem. C* **2007**, *111*, 7411.
(22) Leung, K.; Budzien, J. L. *Phys. Chem. Chem. Phys.* **2010**, *12*, 6583.
(23) Tang, W.; Sanville, E.; Henkelman, G. *J. Phys.: Condens. Matter* **2009**, *21*, 084204.
(24) Wang, Y. X.; Nakamura, S.; Ue, M.; Balbuena, P. B. *J. Am. Chem. Soc.* **2001**, *123*, 11708.
(25) Grimme, S. *J. Comput. Chem.* **2006**, *27*, 1787.
(26) Nishida, T.; Nishikawa, K.; Fukunaka, Y. *ECS Trans.* **2008**, *6*, 1.
(27) Hayamizu, K.; Aihara, Y.; Arai, S.; Martinez, C. G. *J. Phys. Chem. B* **1999**, *103*, 519.
(28) Skundin, a. M.; Grigor'eva, O. Y.; Kulova, T. L.; Pouchko, S. V. *J. Solid State Electrochem.* **2003**, *8*, 11.
(29) Takeuchi, M.; Kameda, Y.; Umebayashi, Y.; Ogawa, S.; Sonoda, T.; Ishiguro, S. I.; Fujita, M.; Sano, M. *J. Mol. Liq.* **2009**, *148*, 99.
(30) Seward, R. P.; Vieira, E. C. *J. Phys. Chem.* **1958**, *62*, 127.
(31) Reynier, Y.; Graetz, J.; Swan-Wood, T.; Rez, P.; Yazami, R.; Fultz, B. *Phys. Rev. B* **2004**, *70*, 174304.
(32) Shigeto, S.; Hamaguchi, H.-o. *Chem. Phys. Lett.* **2006**, *427*, 329.
(33) Burba, C. M.; Frech, R. *J. Phys. Chem. B* **2005**, *109*, 15161.
(34) Chernyak, Y.; Clements, J. H. *J. Chem. Eng. Data* **2004**, *49*, 1180.
(35) Du, W. M.; Li, G.; Cummins, H. Z.; Fuchs, M.; Toulouse, J.; Knauss, L. A. *Phys. Rev. E* **1994**, *49*, 2192.
(36) Kresse, G.; Furthmüller, J. *Phys. Rev. B* **1996**, *54*, 11169.
(37) Kresse, G.; Joubert, D. *Phys. Rev. B* **1999**, *59*, 1758.
(38) Blöchl, P. E. *Phys. Rev. B* **1994**, *50*, 17953.